Plant, Cell and Environment (2002) **25,** 1383–1398

The Ball–Berry–Leuning and Tardieu–Davies stomatal models: synthesis and extension within a spatially aggregated picture of guard cell function

R. C. DEWAR

Unité de Bioclimatologie, INRA Centre de Bordeaux, BP81, 33883 Villenave d'Ornon, France

ABSTRACT

A new model of stomatal conductance is proposed which combines the essential features of the Ball–Berry–Leuning (BBL) and Tardieu–Davies (TD) models within a simple spatially aggregated picture of guard cell function. The model thus provides a coherent description of stomatal responses to both air and soil environments. The model also presents some novel features not included in either the BBL or TD models: stomatal sensing of intercellular (rather than leaf surface) CO_2 concentration; an explanation of all three observed regimes (A, B and C) of the stomatal response to air humidity (Monteith *Plant, Cell and Environment* 18, 357–364, 1995); incorporation of xylem embolism; and maintenance of hydraulic homeostasis by combined hydraulic and chemical signalling in leaves (in which leaf epidermal hydraulic conductivity plays a key role). Significantly, maintenance of hydraulic homeostasis in the model does not require a direct feedback signal from xylem embolism, the predicted minimum leaf water potential being independent of xylem hydraulic conductivity. It is suggested that stomatal regulation through combined hydraulic and chemical signalling in leaves and/or roots provides a general mechanism enabling plants to maintain their water potentials above a minimum value. Natural selection of the key stomatal parameters would then set the minimum potential to a specific value determined by the most vulnerable plant process under water stress (e.g. cell growth, protein synthesis or xylem cavitation), depending on species and growth conditions.

Key-words: abscisic acid; embolism; guard cell; model; stomatal conductance.

INTRODUCTION

Empirical models of stomatal conductance play an important scientific role in summarizing commonly observed trends in stomatal behaviour, and thus guiding the formulation of more mechanistic models. One aim of the latter is to explain, from a mechanistic standpoint, not just the common trends but also the observed departures from those trends, with a view to extending the range of validity of empirical models. The objective of this study is to extend the range of validity of two previously published empirical models (Tardieu & Davies 1993; Leuning 1995), by combining them within a simple spatially aggregated model of guard cell function (based on Dewar 1995).

Correspondence: Roderick C. Dewar. Fax: + 33 (0)5 57 12 24 20; e-mail: dewar@bordeaux.inra.fr

Ball–Berry–Leuning model

The empirical model of Ball, Woodrow & Berry (1987), as modified by Leuning (1990, 1995), states that

$$g = g_0 + \frac{a_1 A_n}{(c_s - \Gamma)\left(1 + \frac{D_s}{D_0}\right)} \quad (1)$$

where g is the stomatal conductance for CO_2 diffusion, A_n is the net leaf CO_2 assimilation rate, D_s and c_s are the vapour pressure deficit (VPD) and CO_2 concentration at the leaf surface, respectively, Γ is the CO_2 compensation point, g_0 is the value of g at the light compensation point, and a_1 and D_0 are empirical coefficients.

This model encapsulates two empirical trends reported in the literature. First, through the correlation between g and A_n, Eqn 1 predicts that the ratio $(c_i - \Gamma)/(c_s - \Gamma)$ (where c_i is the leaf intercellular CO_2 concentration) is largely independent of leaf irradiance and c_s (Wong, Cowan & Farquhar 1979) except near the light and CO_2 compensation points, and declines linearly as D_s increases (Morison & Gifford 1983; Leuning 1995). Secondly, through the relation $E = 1{\cdot}6\, gD_s$ for the transpiration rate, the hyperbolic function of D_s in Eqn 1 is equivalent to a linear decline of g with increasing E (Dewar 1995; Leuning 1995), consistent with the commonly observed behaviour referred to as regime A by Monteith (1995) in his review of stomatal responses to air humidity. Equation 1 can also mimic Monteith's (1995) regime B, in which E decreases at higher VPD (Dewar 1995; Leuning 1995).

The main limitation of the Ball–Berry–Leuning (BBL) model is that it does not describe stomatal closure under soil drying. Also, the factor $A_n/(c_s - \Gamma)$ is inconsistent with the experiments of Mott (1988) showing that stomata sense c_i, not c_s. Mott found that the stomata of sunflower (*Helianthus annuus* L.) and cocklebur (*Xanthium strumarium* L.)

closed when c_i was increased at fixed c_s; under these conditions Eqn 1 would predict stomatal opening rather than closure. Furthermore, in principle the predicted value of g could become negative below the light compensation point (when A_n is negative). Finally, the BBL model does not predict Monteith's (1995) regime C, where g is relatively insensitive to VPD in very moist air.

Tardieu–Davies model

Soil drying experiments on maize (*Zea mays* L) led Tardieu & Davies (1993) to formulate a model of stomatal response to soil water deficit involving combined hydraulic and chemical signalling through abscisic acid (ABA). According to the Tardieu–Davies (TD) model,

$$g = g_{min} + (g_{max} - g_{min})\exp\{-[ABA]\beta\exp(\delta\psi_f)\} \quad (2)$$

where g_{min} and g_{max} are the minimum and maximum stomatal conductances, respectively, [ABA] is the xylem ABA concentration, β (chosen here to be positive) is the basal sensitivity of stomatal conductance to [ABA] at zero foliage water potential ($\psi_f = 0$), and δ (negative value) describes the increase in stomatal sensitivity to [ABA] as ψ_f falls (Tardieu & Davies 1992). ABA was assumed to be produced by the roots at a rate proportional to root water potential, and diluted in the transpiration stream.

As Tardieu & Davies (1993) showed, their model explains two commonly observed and contrasting behaviours of the diurnal minimum foliage water potential ($\psi_{f,min}$). First, when $\delta < 0$ the predicted $\psi_{f,min}$ changes little with the soil water reserve or the soil-to-plant hydraulic conductivity. This phenomenon, called hydraulic homeostasis (or isohydric behaviour), has been observed in many plant species including trees (Oren *et al*. 1999; Magnani, Mencuccini & Grace 2000). Hydraulic homeostasis is somewhat analogous to the homeostatic behaviour of c_i/c_s in the absence of water stress (incorporated in the BBL model but not in the TD model). Secondly, if the interaction between hydraulic and chemical signals is absent ($\delta = 0$), isohydric behaviour is replaced by a marked decrease in $\psi_{f,min}$ in droughted plants (anisohydric behaviour), as observed in sunflower and other species (Tardieu, Lafarge & Simonneau 1996; Tardieu & Simonneau 1998).

It has been proposed that the homeostatic value of $\psi_{f,min}$ in isohydric woody species lies close to the threshold potential for catastrophic xylem failure due to runaway cavitation (Tyree & Sperry 1988), reflecting an optimization strategy of maximum leaf gas exchange that would involve some loss of xylem conductivity (Jones & Sutherland 1991). In their modelling study, Jones & Sutherland (1991) also examined a second possibility, that $\psi_{f,min}$ coincides with the onset of xylem embolism, reflecting a more conservative (cavitation-avoidance) strategy.

However, in coupling Eqn 2 to a description of soil-to-leaf water flux, Tardieu & Davies (1993) did not incorporate the possible effects of xylem embolism and assumed a fixed root-to-leaf hydraulic conductivity. Therefore, the possible role of hydraulic/chemical signals in regulating xylem embolism has yet to be explored by modellers. The relevance of root chemical signals to stomatal regulation in large woody species has been questioned, because of the long transport time from roots to the stomata (Schulze 1991). This criticism is misplaced in the case of the TD model, where the sensitivity of g to the root signal (ABA) is modulated by short-term changes in foliage water potential (Eqn 2). Nevertheless, it has been suggested that rapid stomatal closure in response to shoot xylem cavitation may instead involve hydraulic and/or chemical signals localized in leaves (Salleo *et al*. 2000; Hubbard, Ryan & Sperry 2001).

Therefore, a possible extension of the TD model would be to incorporate xylem embolism and the potential regulatory role of leaf hydraulic and chemical signals, as an alternative or in addition to root signals. Indeed, Tardieu & Davies (1993) emphasized that their model contained many oversimplifications, but suggested that combined hydraulic/chemical feedback regulation could provide a base for further models.

Objectives

In a previous paper (Dewar 1995) the BBL model was interpreted mechanistically in terms of a simple spatially aggregated picture of guard cell function. The main objective of the present paper is to propose a more complete description of stomatal behaviour than either the BBL or TD models alone, based on an extension of the guard cell model (Dewar 1995) to incorporate a role for chemical signalling. The specific aims are:

1 to combine the essential features of the BBL and TD models (Eqns 1 & 2) within a common mechanistic framework;
2 to remove the shortcomings of the BBL model with respect to the factor $A_n/(c_s - \Gamma)$;
3 to extend the TD model to include leaf as well as root chemical signals;
4 to couple the new model to a simple water balance scheme involving xylem embolism;
5 to compare the generic behaviour of the new model with that of the BBL and TD models; and
6 to explore the roles played by root and/or leaf hydraulic and chemical signals in regulating leaf water potential and xylem embolism.

The structure of the paper is as follows. The next section presents the assumptions of the guard cell model, leading to a new expression for the steady-state stomatal conductance (g) in terms of net leaf CO_2 assimilation (A_n), leaf intercellular CO_2 concentration (c_i), leaf xylem ABA concentration ([ABA]) and leaf epidermal water potential (ψ_e) (aims 1–2). Then the assumptions regarding the ABA and water balances, including xylem embolism, are presented (aims 3–4). The behaviour of the model is then examined with regard to the stomatal response to VPD (regimes A–C), and regulation of the c_i/c_s ratio and leaf epidermal water

potential (ψ_e) (aim 5). Finally, the implications of the model for the stomatal regulation of xylem embolism are discussed in the light of these results (aim 6).

GUARD CELL MODEL ASSUMPTIONS (AIMS 1–2)

Figure 1 depicts the overall structure of the model. All conductances and fluxes are expressed per unit leaf area. Symbol definitions and default parameter values are given in Tables 1 and 2, respectively.

Stomatal mechanics

It has been shown both experimentally and theoretically that stomatal aperture is a linear combination of the turgor pressures of the guard cells and their adjoining subsidiary cells, with subsidiary cell turgor having a greater mechanical influence than guard cell turgor (Edwards, Meidner & Sheriff 1976; Wu, Sharpe & Spence 1985; Sharpe, Wu & Spence 1987). The present model, however, considers the relationship of leaf stomatal conductance to the mean turgor pressures of the guard cells and the bulk leaf epidermis (Dewar 1995), which are assumed to have the same mechanical influence on g (but opposite in sign):

$$g = \begin{cases} \chi(P_g - P_e) & \text{if } P_g > P_e \\ 0 & \text{otherwise'} \end{cases} \quad (3a)$$

where g is the leaf conductance for CO_2 diffusion, P_g and P_e are the mean turgor pressures of the guard cells and bulk leaf epidermis, respectively, and χ is a mechanical coefficient. In contrast to the local description of stomatal mechanics involving the mechanical advantage of subsidiary cells, Eqn 3a represents a spatially averaged description. These two descriptions should be considered not as logically exclusive alternatives but rather as potentially equivalent descriptions on different spatial scales.

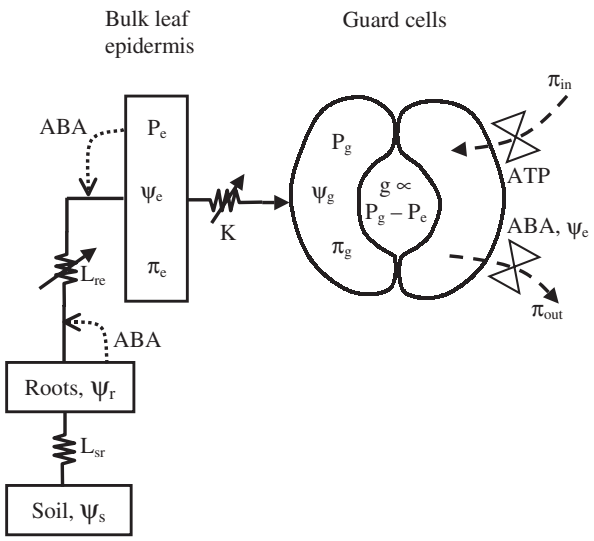

Figure 1. Schematic representation of the guard cell model. See Table 1 for notation. Solid lines represent water fluxes. Broken arrows (right) represent fluxes of osmotica and (left) synthesis of ABA. Osmotic fluxes into (respectively, out of) the guard cells are regulated by ATP (respectively, ABA and leaf epidermal water potential).

As shown in Appendix 1, the two descriptions may be reconciled in principle if it is supposed that the guard/subsidiary cell complex is coupled mechanically to the rest of the epidermis (cf. Meidner & Edwards 1975). Equation 3a is qualitatively consistent with the expectation that the mechanical influence of epidermal cells declines with distance from the guard cell (Stålfelt 1966). Quantitatively however, Eqn 3a represents a working hypothesis whose mechanistic justification would require a scaling-up analysis of cell pressure–volume relations across the epidermis. The main reason for adopting Eqn 3a in this study, as previously (Dewar 1995), is that it is mathematically consistent with the empirical BBL and TD models (as shown below), a 'top-down' philosophy that is reflected in the opening sentence of the Introduction. In contrast, Appendix 2 shows that spatially explicit models describing the known mechanical advantage of subsidiary cells, as currently formulated – specifically, the model of Haefner, Buckley & Mott (1997) which incorporates hydraulic interactions across the leaf – are not yet fully consistent with the BBL and TD models. A spatially explicit 'bottom-up' explanation of the BBL and TD models may require a comprehensive description of mechanical, osmotic and hydraulic interactions across the leaf (see Appendix 2 for further details). This lies outside the scope of the present study.

The turgor pressures of the guard cells and leaf epidermis are calculated from the corresponding water potentials (ψ_g and ψ_e) and osmotic pressures (π_g and π_e):

$$P_g = \begin{cases} \psi_g + \pi_g & \text{if } \psi_g > -\pi_g \\ 0 & \text{otherwise} \end{cases} \quad (3b)$$

and

$$P_e = \begin{cases} \psi_e + \pi_e & \text{if } \psi_e > -\pi_e \\ 0 & \text{otherwise} \end{cases} \quad (3c)$$

The epidermal osmotic pressure (π_e) is assumed to be constant.

Peristomatal transpiration

Previous studies have suggested that evaporation of water into substomatal cavities occurs mainly in the vicinity of the guard cells (e.g. Meidner 1975; Meidner & Edwards 1975; Tyree & Yianoulis 1980). This so-called peristomatal transpiration implies that the water potential difference between the bulk leaf epidermis and the guard cells is proportional to the transpiration rate (E):

$$\Delta\psi = \psi_e - \psi_g = \frac{E}{K}, \quad (4a)$$

where K is the hydraulic conductivity between the bulk leaf epidermis and the guard cells (Dewar 1995). In the default

Table 1. Symbol definitions and units

Symbol	Definition (relevant equations)	Units
a	ABA sequestration rate (8)	mol H_2O m^{-2} s^{-1}
a_1	Parameter combination (7b)	dimensionless
[ABA]	Leaf xylem ABA concentration (8)	mol ABA m^{-3}
A_n	Leaf net CO_2 assimilation rate (10b, c)	mol CO_2 m^{-2} s^{-1}
b	Soil characteristic (9c)	dimensionless
c_i, c_s	Leaf intercellular, surface CO_2 partial pressures	mol CO_2 (mol air)$^{-1}$
d, d_{min}	Ion diffusion rate, minimum value (5a, d)	s^{-1}
D_s	Water vapour partial pressure deficit at leaf surface	dimensionless
D_0	Parameter combination (7c)	dimensionless
E	Leaf transpiration rate (6c)	mol H_2O m^{-2} s^{-1}
g	Stomatal conductance (7a)	mol CO_2 m^{-2} s^{-1}
g_x	Carboxylation conductance (10c)	mol air m^{-2} s^{-1}
g_0	Value of g at light compensation point (1)	mol CO_2 m^{-2} s^{-1}
J_w	Xylem water flux (9a)	mol H_2O m^{-2} s^{-1}
K, K_{max}	Leaf e $\rightarrow$ g hydraulic conductivity, maximum (4b)	mol H_2O m^{-2} s^{-1} MPa^{-1}
L_{re}, L_{max}	Xylem hydraulic conductivity, maximum (9b)	mol H_2O m^{-2} s^{-1} MPa^{-1}
P_i	Turgor pressure of compartment i = e, g (3b, c)	MPa
Q	Leaf photosynthetically active irradiance (10c)	mol quanta m^{-2} s^{-1}
R_d	Leaf dark respiration rate (10c)	mol CO_2 m^{-2} s^{-1}
R_{re}	Xylem hydraulic resistance, $1/L_{re}$	MPa (mol H_2O)$^{-1}$ m^2 s
R_{sr}, $R_{sr,min}$	Soil-root hydraulic resistance, minimum value (9c)	MPa mol^{-1} H_2O m^2 s
V_w	Partial molal volume of water	m^3 mol^{-1} H_2O
α	Photochemical efficiency (10c)	mol CO_2 mol^{-1} quanta
β	ABA sensitivity parameter (2)	m^3 mol^{-1} ABA
δ	ABA sensitivity parameter (2)	MPa^{-1}
μ	Ion pumping coefficient (5c)	MPa mol^{-1} CO_2 m^2 s
Γ	CO_2 compensation point (1)	dimensionless
χ	Stomatal mechanical coefficient (3a)	mol H_2O m^{-2} s^{-1} MPa^{-1}
$\Delta\pi$	Osmotic pressure gradient $\pi_g - \pi_e$ (5b)	MPa
$\Delta\psi$	Water potential gradient $\psi_e - \psi_g$ (4a)	MPa
λ_i	ABA synthesis constants for compartments i = e, r	mol ABA MPa^{-1} m^{-2} s^{-1}
π_{in}	Rate of active ion pumping into guard cells (5a, c)	MPa s^{-1}
π_{out}	Rate of ion diffusion out of guard cells (5a)	MPa s^{-1}
π_i	Osmotic pressure of compartment i = e, g	MPa
Ω	Parameter combination (A3.8)	MPa
ψ_i	Water potential of compartment i = e, g, r, s	MPa
ψ_{smax}	Value of ψ_s at field capacity (9c)	MPa
ψ_{tK}, ψ_{xK}	Threshold potentials for decline in K (4b)	MPa
ψ_{tL}, ψ_{xL}	Threshold potentials for decline in L_{re} (9b)	MPa

Compartment labels: e = bulk leaf epidermis, g = guard cells, r = roots, s = soil. m^2 refers to leaf area.

version of the model, K is assumed fixed at its maximum value (K_{max}). However, a later section will examine the hypothesis that K declines as ψ_e falls, describing the effect of local leaf dehydration on membrane hydraulic conductivity. A simple ramp function will be assumed:

$$K = \begin{cases} K_{max} & \text{if } \psi_e > \psi_{tK} \\ K_{max}(\psi_e - \psi_{xK})/(\psi_{tK} - \psi_{xK}) & \text{if } \psi_{xK} < \psi_e < \psi_{tK} \\ 0 & \text{if } \psi_e < \psi_{xK} \end{cases} \quad (4b)$$

in which ψ_{tK} is the threshold potential at which K starts to decline, and ψ_{xK} is the value of ψ_e at which K falls to zero.

Guard cell solute balance

It is assumed that ions are actively pumped from epidermal cells to the guard cells at a rate denoted by π_{in}. In addition, guard cell solutes are assumed to diffuse back to epidermal cells at a rate π_{out} that is proportional to the difference in osmotic pressures, $\Delta\pi = \pi_g - \pi_e$. The rate of change of the guard cell osmotic pressure is therefore

$$\frac{d\pi_g}{dt} = \pi_{in} - \pi_{out} = \pi_{in} - d(\pi_g - \pi_e), \quad (5a)$$

where d is a diffusion rate coefficient. In the steady state,

$$\Delta\pi \equiv \pi_g - \pi_e = \frac{\pi_{in}}{d} \text{ (steady state)} \quad (5b)$$

It is assumed that the active ion loading rate π_{in} is proportional to the local (guard cell) free energy pool, which is itself assumed to be proportional to the driving force for the CO_2 reduction cycle in mesophyll chloroplasts (in the form of ATP and NADPH). The underlying assumption here is that ATP dynamics in the guard cells and mesophyll cells involve two analogous sets of reactions running in

Table 2. Parameter values. See Table 1 for definitions

Parameter	Default value	Source/comments
a	1×10^{-4} mol H_2O m^{-2} s^{-1}	after Tardieu & Davies (1993)
a_1	6	after Leuning (1995)
b	6	illustrative
c_s	350×10^{-6}	illustrative
D_s	0·03	3 kPa, illustrative
D_0	0·0167	1·67 kPa, after Leuning (1995)
g_x	0·05 mol CO_2 m^{-2} s^{-1}	Dewar (1995)
L_{max}	$6{\cdot}67 \times 10^{-3}$ mol H_2O m^{-2} s^{-1} MPa^{-1}	Saugier & Katerji (1991)
Q	10000×10^{-6} mol quanta m^{-2} s^{-1}	saturating light
R_d	0·0 mol CO_2 m^{-2} s^{-1}	assumed zero for simplicity
$R_{sr,min}$	0·1 MPa mol^{-1} H_2O m^2 s	illustrative
V_w	18×10^{-6} m^3 mol^{-1} H_2O	dilute solution at 20 °C
α	0·05 mol CO_2 mol^{-1} quanta	Dewar (1995)
β	$1{\cdot}48 \times 10^{-4}$ m^3 mol^{-1} ABA	after Tardieu & Davies (1993)
δ	–2 MPa^{-1}	after Tardieu & Davies (1993)
λ_e, λ_r[a]	1·0, 4·0 μmol ABA MPa^{-1} m^{-2} s^{-1}	after Tardieu & Davies (1993)
ψ_s	–0·3 MPa	illustrative
ψ_{smax}	–0·02 MPa	illustrative
ψ_{tK}, ψ_{xK}[b]	–1, –2 MPa	illustrative
ψ_{tL}, ψ_{xL}	–1, –3 MPa	Jones & Sutherland (1991)

[a]Values when ABA synthesis switched on (zero otherwise).
[b]For variable K ($K = K_{max}$ by default). The value of K_{max} is not given explicitly, but is implicit in the value of D_0 (see Eqn 7c).

parallel (Zeiger, Farquhar & Cowan 1987; Kearns & Assmann 1993). This assumption also forms the basis of the stomatal model of Farquhar & Wong (1984). A convenient measure of the mesophyll free energy pool is the ratio $(A_n + R_d)/c_i$, where A_n is the net leaf CO_2 assimilation rate and R_d is the dark respiration rate, $A_n + R_d$ being the rate of gross photosynthesis (e.g. Thornley & Johnson 1990; p. 225, eqn 9·7e). Thus,

$$\pi_{in} = \mu \frac{A_n + R_d}{c_i}, \tag{5c}$$

where μ is an empirical loading rate constant. Although π_{in} has been interpreted here as an influx of osmotica from outside the guard cell, this does not exclude the possibility that a component of π_{in} may involve guard cell sucrose metabolism (Talbott & Zeiger 1998). It should be stressed, however, that Eqn 5c is largely empirical and that the detailed nature of the underlying mechanisms, and their relationship to guard cell ATP, lies outside the immediate scope of this study.

It is assumed that ABA regulates stomatal conductance by stimulating the rate of ion diffusion out of the guard cells (d), and that this effect is enhanced as the epidermal water potential (ψ_e) falls. In anticipation of Eqn 2, an exponential response is assumed:

$$d = d_{min} \exp\{[\mathrm{ABA}]\beta \exp(\delta\psi_e)\}, \tag{5d}$$

where d_{min} is the minimum diffusion rate, [ABA] is the leaf xylem concentration of ABA, β (positive value) is the basal sensitivity of ion diffusion to [ABA] at zero leaf water potential ($\psi_e = 0$), and δ (negative value) describes the increase in the sensitivity of ion diffusion to [ABA] as ψ_e falls. It has been suggested that the apparent interaction between foliage water potential and [ABA] reflects the effect of xylem sap pH on the partitioning of ABA between guard cells and mesophyll cells (Wilkinson & Davies 1997).

Steady-state conductance

The above assumptions may be combined to derive an expression for the steady-state stomatal conductance. For turgor pressures in the normal operating regime $P_g > P_e > 0$, the turgor difference $\Delta P = P_g - P_e$ which determines g (Eqn 3a) can be decomposed into hydraulic ('hydropassive') and osmotic ('hydroactive') components (Eqns 3b & 3c):

$$g = \chi(\Delta\pi - \Delta\psi), \tag{6a}$$

where $\Delta\psi$ and $\Delta\pi$ are given by Eqns 4a and 5b, respectively, leading to

$$g = \chi\left(\frac{\pi_{in}}{d} - \frac{E}{K}\right) \tag{6b}$$

Equation 6b is consistent with the empirical hydraulic feedback relationship $g/g_m = 1 - E/E_m$ (Monteith 1995; regime A), and provides a mechanistic interpretation of the empirical parameters g_m and E_m as $g_m = \chi\pi_{in}/d$ and $E_m = K\pi_{in}/d$.

For example, the form of Eqn 6b suggests a possible mechanistic interpretation of Monteith's (1995) re-analysis of data from experiments by Turner, Schulze & Gollan (1985) on stomatal responses in *Helianthus annuus*. In Monteith's re-analysis, the fitted value of g_m increased with extractable soil water content (EWC) over the range 2–8% but was approximately independent of EWC above 8%; Eqn 6b suggests that this behaviour could reflect ABA-induced changes in the ion diffusion rate d over the range 2–8% EWC. In contrast, Monteith (1995) found that the

fitted value of E_m increased over the entire experimental range of EWC (2–94%); this would then be consistent with Eqn 6b if the leaf hydraulic conductivity K increased with EWC over the entire range 2–94%. Variation in K with soil water content might be modelled through the intermediary of leaf water potential, as in Eqn 4b, possibly representing an effect of leaf water status on cell membrane hydraulic conductivity. The implications of a variable K will be explored in a later section.

A more detailed expression for g follows by combining Eqn 6b with the expression for the transpiration rate,

$$E = 1{\cdot}6gD_s, \tag{6c}$$

and by substituting Eqns 5c and 5d for π_{in} and d. After rearrangement, we find

$$g = \frac{a_1(A_n + R_d)}{c_i\left(1 + \dfrac{D_s}{D_0}\right)} \exp\{-[\mathrm{ABA}]\beta\exp(\delta\psi_e)\}, \tag{7a}$$

where the coefficients a_1 and D_0 are given in terms of the guard cell parameters by

$$a_1 = \frac{\chi\mu}{d_{\min}}, \tag{7b}$$

$$D_0 = \frac{K}{1{\cdot}6\chi}. \tag{7c}$$

Equation 7a–7c is the central result of the paper; the steady-state stomatal conductance is the product of two factors encapsulating, respectively, the essential features of the BBL and TD models (cf. aim 1).

It will also be noted (cf. aim 2) that in replacing the factor $A_n/(c_s - \Gamma)$ of the BBL model by $(A_n + R_d)/c_i$, Eqn 7a is consistent with stomatal sensing of c_i (and not c_s), and correctly predicts stomatal closure when c_i is increased at fixed c_s (Mott 1988). The factor $(A_n + R_d)/c_i$ also predicts that g remains positive at and below the light and CO_2 compensation points and, moreover, leads to a reduction in the number of model parameters (R_d in place of g_0 and Γ). Leuning (1995) found that the values of a_1 and D_0 obtained from empirical fits of the BBL model were negatively correlated, a possible explanation for which is suggested by Eqns 7b and 7c in terms of variation in the mechanical coefficient χ.

Finally, note that in the new model the stomatal response to air humidity (D_s) occurs through two mechanisms inherited, respectively, from the BBL and TD models: (i) hydraulic feedback via peristomatal transpiration, giving the factor $1/(1 + D_s/D_0)$ in Eqn 7a, and (ii) modulation of the stomatal sensitivity to [ABA] via changes in ψ_e (for $\delta < 0$). In experiments by Assmann, Snyder & Lee (2000), stomatal conductance was as sensitive to D_s in ABA-deficient and ABA-insensitive mutants of *Arabidopsis* as in wild-type plants, appearing to rule out an obligate role for ABA in the stomatal response to air humidity, and implicating the involvement of a non-ABA-related mechanism. By combining the BBL and TD models, the new model includes both non-ABA- and ABA-related feedback mechanisms – respectively, peristomatal transpiration and sensitizing of stomata to ABA – with the former (latter) dominating when the parameter D_0 is small (large). Referring to Eqn 7c, the relative importance of these two mechanisms would be affected by the leaf epidermal-to-guard cell hydraulic conductivity (K).

ABA AND WATER BALANCE ASSUMPTIONS (AIMS 3–4)

Tardieu & Davies (1993) considered root-synthesized ABA only. The present model allows for the possibility that ABA synthesis occurs in the roots and/or the leaves (Hartung & Davies 1991). Extrapolating the approach of Tardieu & Davies (1993), it is assumed that the ABA synthesis rates in both roots and leaves increase linearly as their respective water potentials decrease. Although a linear relationship is the simplest assumption here, and a non-linear relationship may be more realistic (Pierce & Raschke 1981), the precise form of this relationship does not affect the main conclusions of the present study.

In the steady state, the leaf xylem ABA concentration is the balance between total ABA synthesis, dilution by the water flux (J_w), and an effective ABA sequestration rate (a):

$$[\mathrm{ABA}] = \frac{-\lambda_r\psi_r - \lambda_e\psi_e}{V_w(J_w + a)}, \tag{8}$$

where λ_r and λ_e are root and leaf ABA synthesis coefficients (positive values), and V_w is the partial molal volume of water. This formulation allows for the possibilities that ABA is synthesized by the leaves only ($\lambda_r = 0$, $\lambda_e > 0$, the default case), by roots only ($\lambda_r > 0$, $\lambda_e = 0$), or by both ($\lambda_r > 0$, $\lambda_e > 0$) (cf. aim 3). Equation 8 gives the steady-state value of [ABA]; this may be a reasonable approximation to the dynamic value for the case of leaf-synthesized ABA ($\lambda_r = 0$, $\lambda_e > 0$), but will be less accurate in the case of root-synthesized ABA ($\lambda_r > 0$) on account of lags due to the transport time from roots to the stomata (days for some trees). Such dynamic effects lie outside the scope of the present study.

The soil-to-leaf water flux (J_w) is described by an Ohm's law analogue:

$$J_w = \frac{\psi_s - \psi_e}{R_{sr} + R_{re}}, \tag{9a}$$

where ψ_s is the soil water potential, and R_{sr} and R_{re} are the soil-to-root and root-to-leaf epidermis hydraulic resistances, respectively. The value of R_{re} is assumed to increase as xylem vessels become embolized (cf. aim 4). Following Jones & Sutherland (1991), a simple ramp function is used to describe the relationship between the xylem hydraulic conductivity $L_{re} = 1/R_{re}$ and leaf epidermal water potential (cf. Eqn 4b):

$$L_{re} = \begin{cases} L_{\max} & \text{if } \psi_e > \psi_{tL} \\ L_{\max}(\psi_e - \psi_{xL})/(\psi_{tL} - \psi_{xL}) & \text{if } \psi_{xL} < \psi_e < \psi_{tL} \\ 0 & \text{if } \psi_e < \psi_{xL} \end{cases} \tag{9b}$$

in which L_{max} is the maximum root-to-leaf hydraulic conductivity, ψ_{fL} is the threshold potential at which L_{re} starts to decline and ψ_{xL} is the value of ψ_e at which L_{re} falls to zero. Sperry *et al*. (1998) have discussed a more realistic description of xylem embolism, which could also be implemented in the present model. Equation 9b is adopted here for simplicity. As discussed below, the conclusion of the present study concerning the stomatal regulation of xylem embolism (aim 6) does not depend on the particular function used in Eqn 9b.

The soil-to-root hydraulic resistance (R_{sr}) is given by (e.g. Thornley & Johnson 1990; ch. 15):

$$R_{sr} = R_{sr,min}\left(\frac{\psi_s}{\psi_{smax}}\right)^{2+\frac{3}{b}}, \quad (9c)$$

where $R_{sr,min}$ and ψ_{smax} are, respectively, the minimum soil hydraulic conductivity and maximum soil water potential at field capacity, and b is a dimensionless constant usually lying in the range $2 < b < 18$ and depending on soil type ($b = 2$ for sand, $b = 18$ for clay). The root water potential is then given by

$$\psi_r = \psi_s - R_{rs}J_w. \quad (9d)$$

Steady-state solution

The steady-state solution of the coupled stomatal-xylem system involves finding five unknowns: g, A_n, c_i, [ABA] and ψ_e. The central relationship between these variables is given by the stomatal conductance model (Eqn 7a). A second relationship is given by the expression for [ABA] (Eqn 8), in which J_w and ψ_r are related to ψ_e via Eqns 9a, 9b and 9d. A third relationship is given by the steady-state balance between the rates of xylem water transport and leaf transpiration ($J_w = E$) which, from Eqns 9a and 6c, gives:

$$\frac{\psi_s - \psi_e}{R_{sr} + R_{re}} = 1{\cdot}6gD_s. \quad (10a)$$

Two further relationships are required. These are given by the CO_2 diffusion equation (the 'CO_2 supply function'):

$$A_n = g(c_s - c_i), \quad (10b)$$

and the biochemical relationship between gross photosynthesis ($A_n + R_d$) and the intercellular CO_2 concentration (c_i) (the 'CO_2 demand function'). Among the numerous photosynthesis models available, I chose the simplest for present purposes (Thornley & Johnson 1990; Eqn 9·7i):

$$A_n + R_d = \frac{\alpha Q c_i g_x}{\alpha Q + c_i g_x}, \quad (10c)$$

where α is the photochemical efficiency, Q is leaf photosynthetically active irradiance, and g_x is the carboxylation conductance. Equation 10c ignores photorespiration. The conclusions of the present study do not depend significantly on the particular form of the CO_2 demand function, and alternative forms could be used (e.g. Farquhar, von Caemmerer & Berry 1980; von Caemmerer & Farquhar 1981).

The steady-state solution may then be obtained by numerically solving Eqns 7a, 8 and 10a–10c, although some analytical simplification is possible under the approximation that R_d is negligible compared to A_n (see Eqn 11 below).

Water supply and demand curves

The steady-state solution may be represented graphically (Fig. 2a) as the intersection of two curves describing the dependencies of, respectively, the xylem water flux (J_w, the 'water supply curve') and the leaf transpiration rate (E, the 'water demand curve') on epidermal water potential (ψ_e). The point of intersection of the water supply and demand curves represents the steady state where $J_w = E$ (Eqn 10a). The water supply and demand curves can be constructed by expressing each side of Eqn 10a in terms of ψ_e alone (i.e. after eliminating the other unknowns g, A_n, c_i and [ABA] using the remaining four relationships).

As Fig. 2a shows, the water supply curve (J_w versus ψ_e) falls to zero at $\psi_e = \psi_s$ (zero soil-to-leaf water potential gradient) and $\psi_e = \psi_{xL}$ (complete loss of hydraulic conductivity through xylem embolism). The intermediate point at which J_w has a maximum represents the water potential below which catastrophic xylem failure through runaway cavitation would occur in the absence of stomatal regulation of ψ_e (Tyree & Sperry 1988; Jones & Sutherland 1991).

The shape of the water demand curve (**E versus ψ_e**) reflects the role of ψ_e in regulating the sensitivity of the guard cell ion diffusion rate (d) to ABA, as well as the production and dilution of ABA itself. As ψ_e decreases, increased sensitivity of d to ABA leads to a decline in E (Fig. 2a). When ψ_e approaches ψ_{xL} this decline in E is enhanced by an increase in [ABA] as J_w (and thus ABA dilution) becomes small due to xylem embolism. The hydraulic feedback via peristomatal transpiration does not affect the overall shape of the water demand curve, but instead raises the entire curve as VPD increases, because this feedback is regulated through the epidermal-guard cell water potential difference ($\Delta\psi$) rather than the absolute value of ψ_e.

MODEL BEHAVIOUR (AIM 5)

In this section, I examine the behaviour of the new model with regard to the stomatal response to VPD (regimes A–C), and regulation of the c_i/c_s ratio and foliage water potential (ψ_e), and compare this with the BBL and TD models (aim 5). The results are presented for the default case where ABA is synthesized in the leaves only ($\lambda_e > 0$, $\lambda_r = 0$), and the leaf epidermal hydraulic conductivity (K) is fixed at its maximum value (K_{max}). The value of K_{max} is not given explicitly, but is implicit in the value of D_0 (Eqn 7c). Other parameter values are given in Table 2. A subsequent section will examine the effects on leaf water potential of root versus leaf ABA synthesis and of variable K with a view to gaining theoretical insights into the stomatal regulation of xylem embolism (cf. aim 6).

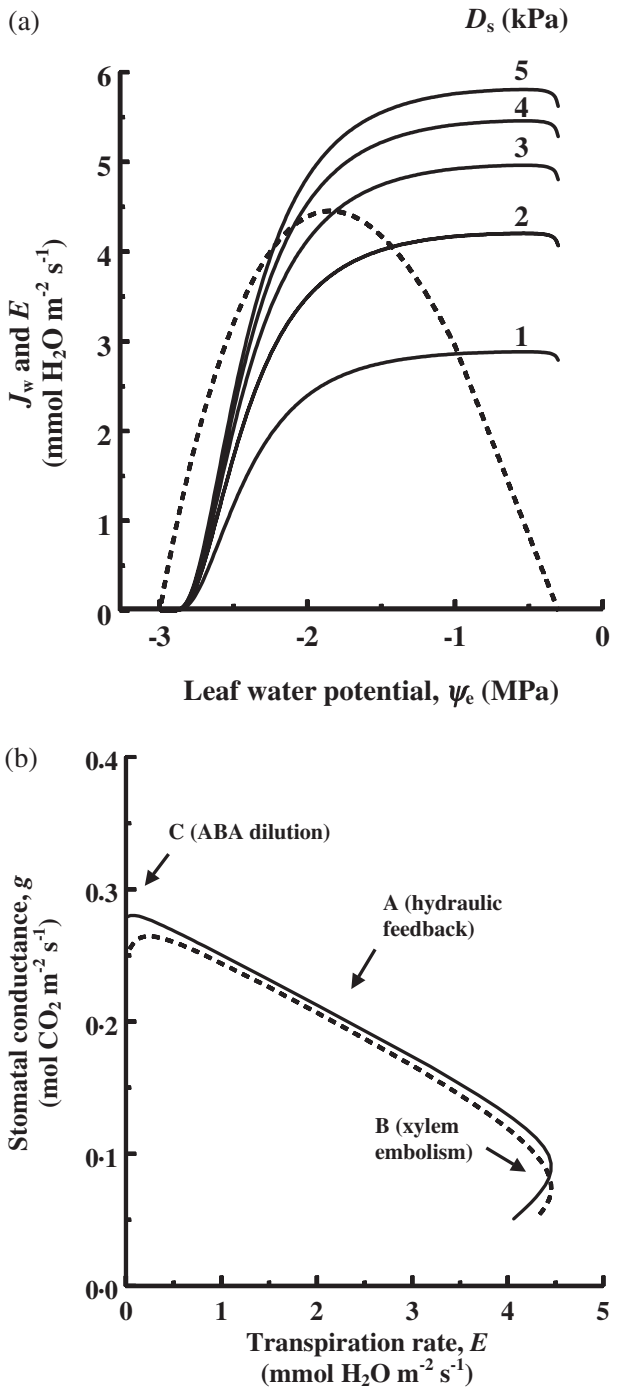

Figure 2. (a) The 'water supply curve' (J_w versus ψ_e, broken line), and the 'water demand curves' (E versus ψ_e, solid lines) at various vapour pressure deficits (D_s), for the default case (ABA synthesis in leaves only, fixed leaf epidermal hydraulic conductivity K). Steady states are given by the points of intersection of the water supply and demand curves. (b) The steady-state relationship between stomatal conductance (g) and E as D_s varies over the range 0·01–5·0 kPa, for ABA synthesis in leaves only (solid line, corresponding to (a)) and roots only (broken line). Three regimes (A, B and C) are predicted (cf. Monteith 1995), which the model explains in terms of, respectively, hydraulic feedback, 'supercritical' xylem embolism, and ABA dilution. Other parameter values are given in Table 2.

Stomatal response to air humidity: regimes A, B and C

Figure 2a illustrates the water demand curves for a range of air humidity deficits (D_s), with other parameter values given in Table 2. As D_s increases, the height of the point of intersection with the water supply curve at first increases, then reaches a peak before decreasing due to the progressive loss of hydraulic conductivity from xylem embolism.

Figure 2b shows the corresponding plot of g against E. Three regimes of behaviour can be identified, similar to the experimentally observed regimes A, B and C reviewed by Monteith (1995). In regime A (moderate values of D_s), g declines linearly with increasing transpiration rate (E). This behaviour reflects the two hydraulic feedback mechanisms through peristomatal transpiration and sensitizing of stomata to ABA. In regime B (high D_s), E decreases as D_s is increased. Farquhar (1978) suggested that such behaviour was a reflection of non-stomatal (cuticular) transpiration. Mott & Parkhurst (1991) suggested that patchy stomatal closure was responsible. The present model provides an additional/alternative explanation in which the decline in E at high D_s is due to xylem embolism (corresponding to steady states lying to the left of the peak in the water demand curve, Fig. 2a). The possibility that regime B might reflect a decline in hydraulic conductance with increasing D_s, caused by xylem cavitation, has been noted previously (Oren *et al*. 1999; Buckley & Mott 2002). The observation by Franks, Cowan & Farquhar (1997) that the short-term stomatal response to VPD in regime B was irreversible (i.e. involved hysteresis) lends indirect support to this explanation (Buckley & Mott 2002).

Monteith (1995) also noted a third regime C at low D_s, less frequently observed perhaps because of experimental difficulties in avoiding condensation. In this regime, stomatal conductance is relatively insensitive to humidity or transpiration rate (e.g. Thomas & Eamus 1999). This regime may be identified with the local maximum in the g–E plot at high humidity (Fig. 2b), and reflects the effect of ABA dilution by the water flux J_w (Eqn 8). ABA dilution is most sensitive to J_w at low J_w (i.e. low D_s) where it dominates the hydraulic feedback effect, resulting in an *increase* in g as E increases at low D_s. The local maximum in g occurs when the dilution and hydraulic feedback effects cancel, resulting in no response of g to humidity. With further increase in E, the hydraulic feedback effect dominates, stomatal closure occurs, and the system passes into regime A. Regime C becomes more pronounced as the ABA sequestration rate (a) tends to zero (data not shown), or when ABA synthesis occurs in the roots (Fig. 2b).

The new model therefore explains not only regimes A (hydraulic feedback) and B (xylem embolism), but also regime C (ABA dilution), and thus extends the range of validity of the BBL model.

Behaviour of c_i/c_s

Let us consider the behaviour of c_i/c_s under the approximation that R_d is negligible compared to A_n, which is reason-

able except in the vicinity of the light or CO_2 compensation points (cf. Fig. 1 in Leuning 1995). This approximation allows c_i/c_s to be calculated analytically. By substituting Eqn 10b into Eqn 7a and re-arranging, we find:

$$\frac{c_i}{c_s} \approx \frac{1}{1+\frac{1}{a_1}\left(1+\frac{D_s}{D_0}\right)\exp\{[\mathrm{ABA}]\beta\exp(\delta\psi_e)\}} \quad (11)$$

(for $R_d << A_n$).

This result predicts that c_i/c_s declines with increasing D_s (Fig. 3) but is independent of Q and c_s (and of the choice of photosynthesis model, Eqn 10c). As Q and c_s approach the light and CO_2 compensation points, respectively, Eqn 11 is replaced by $c_i/c_s = 1$.

Thus, in the absence of water stress, the new model predicts the same generic behaviour of c_i/c_s as the BBL model. Quantitatively, the decline of c_i/c_s with increasing D_s in the new model at low water stress (Fig. 3) would be practically indistinguishable from the negative linear relationship between c_i/c_s and D_s predicted by the BBL model. Thus, use of the factor $(A_n + R_d)/c_i$ overcomes the aforementioned difficulties associated with the factor $A_n/(c_s - \Gamma)$ in the BBL model, while retaining the same qualitative and quantitative behaviour of c_i/c_s in the absence of water stress.

Let us now consider the behaviour of c_i/c_s in the presence of water stress. Experimentally, the observed c_i/c_s ratio sometimes declines under soil drying (Korol *et al*. 1999), although not always (McMurtrie *et al*. 1992). Equation 11 predicts the former response (via the ABA component of the new model). This behaviour is equivalent to a decrease in the apparent slope of the unstressed model (a_1). The new model does not account for the possibility of patchy stomatal closure, corresponding to a constant a_1, a constant c_i/c_s ratio, and a parallel reduction in g and A_n. Leuning (1995) showed that variation of a_1 in the BBL model under water stress would produce a family of curves for c_i/c_s versus D_s that are roughly parallel, whereas patchy stomatal closure would cause c_i/c_s to converge at low D_s and diverge at high D_s, thus suggesting a method of experimentally distinguishing these two modes of stomatal closure under water stress.

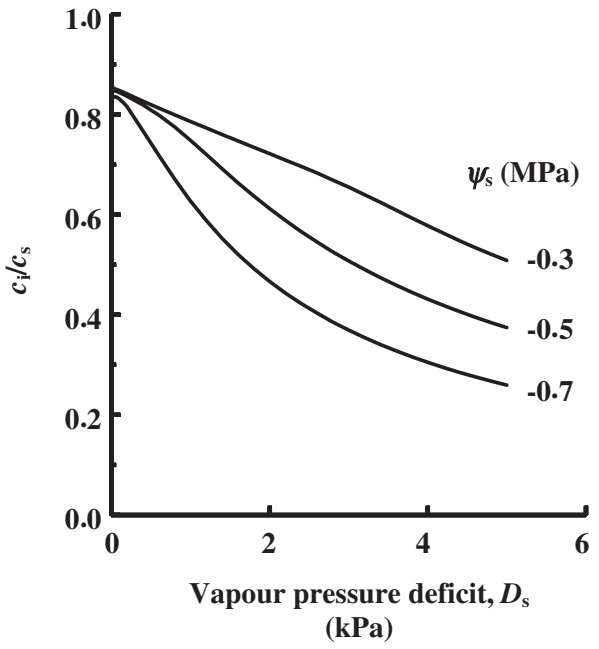

Figure 3. The c_i/c_s ratio as a function of vapour pressure deficit (D_s) at different soil water potentials (ψ_s), for the default case (ABA synthesis in leaves only, fixed leaf epidermal hydraulic conductivity K) corresponding to Fig. 2a. Other parameter values are given in Table 2.

As shown in Fig. 3, the new model predicts a diverging family of curves of c_i/c_s versus D_s under different soil water potentials (ψ_s). This picture is similar to what one would expect from patchy closure in the BBL model, even though patchy closure is not included in the new model. This is because the decrease in the apparent slope of the unstressed model (described by the ABA-dependent factor in Eqn 7a, as inherited from the TD model) is not the same at all values of D_s, being smallest at high ψ_e (low D_s) and greatest at low ψ_e (high D_s) through sensitizing of the stomatal response to ABA. The implication of the new model therefore is that it may not be straightforward to infer the existence of patchy closure under water stress from plots of c_i/c_s versus D_s in the manner suggested by Leuning (1995), because of the ABA × ψ_e interaction.

Regulation of leaf water potential

Figure 4 shows the predicted response of leaf epidermal water potential (ψ_e) to air and soil humidity deficits. As D_s increases, ψ_e at first decreases but then reaches a minimum value ($\psi_{e,min}$) that is insensitive to further increases in D_s (Fig. 4a) and changes little with soil water potential (ψ_s) (Fig. 4b). Therefore the new model, like the TD model, leads to homeostatic regulation of leaf water potential.

What are the key model features that account for this hydraulic homeostasis? To answer this question it is instructive to consider how stomata would have to behave in order to maintain the foliage water potential (ψ_e) strictly constant under variations in D_s and ψ_s ('perfect homeostasis'). From the steady-state balance between water supply and demand,

$$J_w = E = 1{\cdot}6gD_s, \quad (12a)$$

we see that *if* stomatal conductance were inversely proportional to D_s and directly proportional to the supply rate J_w,

$$g = f_\psi \frac{J_w}{D_s}, \quad (12b)$$

(where f_ψ represents any explicit dependence of g on ψ_e) *then* we would have

$$f_\psi = \frac{1}{1{\cdot}6}. \quad (12c)$$

For this hypothetical plant therefore f_ψ and hence ψ_e would be constant under variations in air and soil humidity deficit, and the constant value of ψ_e would depend only on the

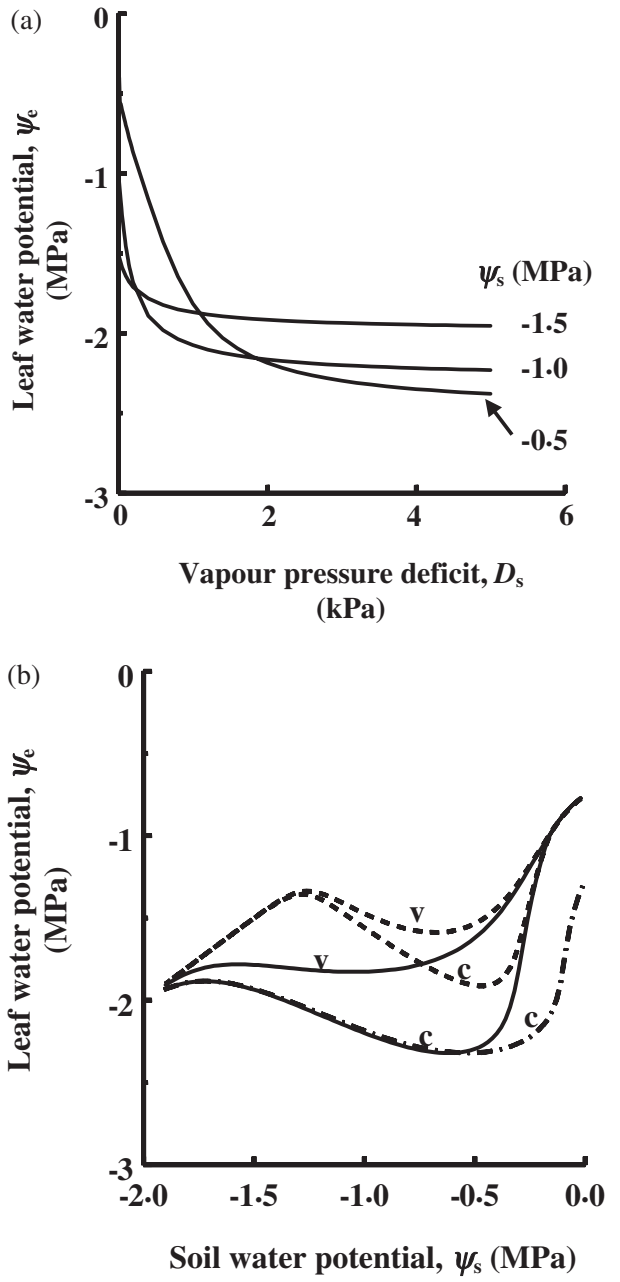

Figure 4. (a) Leaf water potential (ψ_e) as a function of vapour pressure deficit (D_s) at different soil water potentials (ψ_s), for the default case (ABA synthesis in leaves only, fixed leaf epidermal hydraulic conductivity, K). (b) ψ_e as a function of ψ_s at $D_s = 3$ kPa, for ABA synthesis in leaves only (solid curves) and roots only (broken curves), with constant (c) or variable (v) leaf K. In the case of variable K, a ramp function of ψ_e was used (Eqn 4b), which in view of Eqn 7c was applied to parameter D_0. Parameters are given in Table 2. The dot–dash line shows the effect of decreasing the maximum xylem hydraulic conductivity (L_{max}) by a factor of 3 in the default case; this does not affect the minimum value of ψ_e, in accordance with Eqns A3·9 and A3·10 (Appendix 3).

functional form of f_ψ. The new model (Eqn 7a) is not *exactly* of the form required for perfect homeostasis (Eqn 12b). Nevertheless, the humidity function $1/(1 + D_s/D_0)$ in Eqn 7a becomes more nearly proportional to $1/D_s$ as D_s increases. Furthermore, for a given value of ψ_e, there is a strong positive relationship between g and J_w through the effect of ABA dilution (Eqn 8). We conclude that the two key model features accounting for the maintenance of hydraulic homeostasis under variations in air and soil humidities are: (i) hydraulic feedback through peristomatal transpiration, and (ii) xylem ABA dilution by the transpiration stream. These features ensure that an *approximate* homeostasis is maintained, particularly under the moderate to severe air and soil humidity deficits for which hydraulic homeostasis is likely to be of greatest advantage to the plant.

We have identified the link between g and J_w as the key feature underlying hydraulic homeostasis with respect to variation in the soil water reserve. Tardieu & Davies (1993) suggested that the key feature is the ABA × ψ_e interaction, because suppression of this interaction ($\delta = 0$) leads to anisohydric behaviour. In fact there is no real conflict between these two views. As discussed in the following section, homeostasis is still possible when $\delta = 0$, although at an unrealistically low value of $\psi_{e,min}$ (below −100 MPa). Thus, the $g - J_w$ correlation ensures the *possibility* of homeostasis, while the ABA × ψ_e interaction ($\delta < 0$) ensures that the actual value of $\psi_{e,min}$ lies within physiologically reasonable bounds. Varying δ is analogous to changing the functional form of f_ψ in Eqn 12c.

How does the degree of hydraulic homeostasis predicted by the new model compare with that predicted by the TD model? As already mentioned, the air humidity response in the TD model (Eqn 2) occurs entirely through the dependence of g on ψ_e and [ABA], whereas in the new model an additional hydraulic feedback response occurs through the factor $1/(1 + D_s/D_0)$ reflecting the role of peristomatal transpiration. With reference to Eqn 12b *et seq.*, it follows that the value of ψ_e is more stable with respect to changes in D_s in the new model than in the TD model (as may be verified numerically – data not shown). By including the effect of peristomatal transpiration (inherited from the BBL model), the new model maintains hydraulic homeostasis under variations in both air and soil humidity.

Common basis for homeostatic behaviours

As noted in the Introduction, hydraulic homeostasis is analogous to the homeostatic behaviour of c_i/c_s in the absence of water stress. We have seen how the former arises from a positive correlation between g and J_w (via ABA dilution) whereas the latter arises from a positive correlation between g and A_n (via ATP). These two behaviours therefore have a common basis; in either case, approximate homeostasis is maintained through a positive correlation between the diffusive conductance (for H_2O or CO_2) and the corresponding (H_2O or CO_2) flux.

REGULATION OF LEAF WATER POTENTIAL BY LEAF/ROOT CHEMICAL AND HYDRAULIC SIGNALS (AIM 6)

In the previous section it was argued that maintenance of hydraulic homeostasis under variations in air and soil humidity depends on two key features: (i) hydraulic feedback through peristomatal transpiration, and (ii) xylem ABA dilution by the transpiration stream. In this final section I examine more quantitatively how root and/or leaf chemical and hydraulic signals affect the tightness of homeostatic control under soil drying, as well as the actual value of the minimum leaf water potential that is attained (i.e. its dependence on parameters such as δ).

Figure 4b shows how ψ_e depends on soil water potential at fixed VPD, for the default case (ABA synthesized in leaves only, fixed leaf epidermal hydraulic conductivity K), as well as the effects of switching ABA synthesis to the roots and/or allowing K to vary as a function of ψ_e (Eqn 4b). Two main conclusions may be drawn from Fig. 4b: (i) the model is able to maintain a certain degree of hydraulic homeostasis under soil drying, irrespective of whether ABA synthesis occurs in the roots or the leaves, and irrespective of whether K is constant or varies with ψ_e, but (ii) the tightest regulation of ψ_e occurs when K varies with ψ_e (which represents an extra hydraulic feedback), particularly when ABA synthesis occurs in the leaves.

What are the key parameters affecting the minimum leaf water potential ($\psi_{e,min}$) that is attained? The value of $\psi_{e,min}$ corresponds to the lowest turning point in the ψ_e versus ψ_s plot (Fig. 4b). As shown in Appendix 3, an implicit equation may be derived for $\psi_{e,min}$ (Eqn A3·7) in the limit of saturating light ($Q \to \infty$) and under the approximation that the ABA sequestration rate (a, Eqn 8) is small relative to the dilution flux (J_w). Even without solving this equation (which must be done numerically), the analytical form of the equation itself shows us which parameters affect the value of $\psi_{e,min}$, and which parameters do not.

For example, in the default case where ABA is synthesized in leaves only ($\lambda_r = 0$, $\lambda_e > 0$), and in the limit of high VPD ($D_s \to \infty$, corresponding to the lowest possible value of $\psi_{e,min}$), the equation is particularly simple. From Eqns A3·9 and A3·11 (Appendix 3), $\psi_{e,min}$ is given in this case by the value of ψ_e satisfying

$$-\psi_e \exp(\delta\psi_e) = \Omega \tag{13a}$$

where Ω is given by the parameter combination

$$\Omega = \frac{\mu K g_x V_w \exp(-1)}{d_{min}\beta\lambda_e}. \tag{13b}$$

Equation 13a implies that, in the default case, $\psi_{e,min}$ depends on just two factors: δ (ABA-sensitivity parameter) and Ω. Equation 13b shows that Ω depends on (i) the ABA-related parameters d_{min}, β and λ_e (ii) the ATP-related parameters μ and g_x, and (iii) the leaf epidermal hydraulic conductivity (K). Realistic values of $\psi_{e,min}$ of the order of 1–3 MPa are obtained with the parameter values of Table 2 (in which $\delta = -2$ MPa). In contrast, when $\delta = 0$ the value of $\psi_{e,min}$ lies below −100 MPa. Therefore, although hydraulic homeostasis is still possible when $\delta = 0$, the value of $\psi_{e,min}$ is unrealistically low unless $\delta < 0$.

An interesting conclusion that emerges from Eqn 13 is that $\psi_{e,min}$ is independent of the soil-to-root hydraulic conductivity (as found by Tardieu & Davies 1993) as well as the xylem hydraulic conductivity (L_{re}) as illustrated in Fig. 4b. The implication of this conclusion for the stomatal regulation of xylem embolism is discussed below.

DISCUSSION

Synthesis and extension of BBL and TD models

The new model combines the main features of the BBL and TD models within a simple spatially aggregated picture of guard cell function. Mathematically, the new model (Eqn 7a) is simply the product of the BBL and TD models, and so their respective properties combine quasi-independently. This is why the homeostatic behaviours of the c_i/c_s ratio and of leaf water potential are preserved. At the same time, the new model presents four novel features not included in either the BBL or TD models.

First, and most obviously, the new model combines stomatal responses to above-ground factors (from BBL) with responses to soil drying (from TD). Secondly, the model captures all three regimes of the VPD response (Monteith 1995): regime A (hydraulic feedback, from BBL and TD), regime C (ABA dilution, from TD), and regime B (through the inclusion of xylem embolism).

Thirdly, the integration of chemical and hydraulic signals in the TD model has been extended to include (i) leaf ABA synthesis, and (ii) extra hydraulic signals through peristomatal transpiration (from BBL) and leaf epidermal hydraulic conductivity (K). As a result, tighter homeostatic control of leaf water potential is achieved in the new model under variations in VPD (through the extra hydraulic signal from peristomatal transpiration) as well as under soil drying (through the extra coupling of hydraulic and chemical signals via K and leaf ABA).

Fourthly, the factor $(A_n + R_d)/c_i$ avoids the shortcomings of the BBL factor $A_n/(c_s - \Gamma)$. Use of the factor $(A_n + R_d)/c_i$, being more directly related to mesophyll ATP than $A_n/(c_s - \Gamma)$, is also more consistent with the ATP-based stomatal model of Farquhar & Wong (1984), which was developed largely to explain the observed behaviour of c_i/c_s. Thus the new model actually represents a synthesis of three previous models (Farquhar & Wong 1984; Tardieu & Davies 1993; Leuning 1995). As an aside, we note that although the BBL factor $A_n/(c_s - \Gamma)$ mimics regime B at high VPD (due to a reduction in c_i), this behaviour is lost when using $(A_n + R_d)/c_i$, so inclusion of xylem embolism (or some other mechanism such as cuticular transpiration) is then necessary to explain this regime.

Regulation of xylem embolism

It has been suggested that the observed minimum value of ψ_e in woody plants is related to the threshold potential for the onset of xylem cavitation (Tyree & Sperry 1988; Jones & Sutherland 1991; Sperry & Pockman 1993). Subsequently, various authors have suggested a role for chemical and hydraulic signals in the stomatal control of xylem embolism (e.g. Cochard, Bréda & Granier 1996; Salleo *et al*. 2000). Salleo *et al*. (2000) speculated that minor drops in water flow in stem and/or leaf veins caused by cavitation might induce major changes in water potential at the level of guard cells, and/or trigger localized chemical signals such as release of apoplastic ABA or pH changes, leading to stomatal closure.

The present model demonstrates that stomatal regulation of xylem embolism could indeed operate successfully through a combination of changes in leaf epidermal hydraulic conductivity (K, which affects the epidermal-guard cell water potential difference, $\Delta\psi$) and leaf [ABA]. Significantly, it is just this combination of leaf hydraulic and chemical signals which achieves the tightest control of ψ_e in the model. To this extent, the model supports the suggestion of Salleo *et al*. (2000).

However, as was shown in Appendix 3 and as illustrated in Fig. 4b, in the model the minimum leaf water potential ($\psi_{e,min}$) does not depend explicitly on the xylem hydraulic conductivity (L_{re}). As shown in Appendix 3, the key parameters determining $\psi_{e,min}$ include the threshold potentials (ψ_{tK} and ψ_{xK}) defining the vulnerability curve of the leaf epidermal hydraulic conductivity (K, Eqn 4b), and the ABA-related parameters δ, β and λ_e. Although the model does not exclude the possibility that some of these parameters (e.g. λ_e) are linked dynamically to xylem cavitation events, the model suggests that there need be no dynamic link between xylem cavitation and stomatal closure in order to regulate the extent of xylem embolism (cf. Salleo *et al*. 2000). Rather, for a given species the key parameters determining the minimum leaf water potential (e.g. ψ_{tK}, ψ_{xK}, δ, β and λ_e) may simply be selected so as to maintain $\psi_{e,min}$ at a value appropriate to the successful functioning of that species, a value which might imply either some decline in L_{re} (optimization strategy) or avoidance of embolism altogether (conservative strategy) (Jones & Sutherland 1991).

Indeed, the value of $\psi_{e,min}$ in the model need not be related to xylem embolism at all, and might correspond to a threshold level of water status that is critical to some other process sensitive to water stress, such as growth. The suggestion here is that combined hydraulic and chemical signalling in leaves and/or roots provides a general stomatal mechanism by which plants may control their water status independently of the nature of the physiological process which is primarily affected by water stress. The minimum leaf water potential might then be set through natural selection of the key stomatal control parameters (e.g. ψ_{tK}, ψ_{xK}, δ, β and λ_e), at a value determined by the most vulnerable process under water stress, which might be cell growth, protein synthesis, respiration, xylem cavitation, photosynthate translocation or some other process sensitive to water stress, depending on species and growth conditions (Hsiao 1973).

Key model features requiring further critical evaluation

The BBL × TD model (Eqn 7a) and its derivation represent, respectively, a practical proposal for improving the predictive ability of the BBL and TD models, and an underlying theoretical justification of that synthesis in terms of guard cell function. The new model can be criticised on both levels, and this is useful: a stomatal model based on a theoretical description of guard cell function, no matter how crude that description might be, has the advantage that when the model fails at the empirical level, as all models eventually do, the cause of failure can be identified and corrected in a more systematic way than is possible with a purely empirical model (Thornley 1997).

On the practical level, the key feature to be tested experimentally is the multiplicative nature of the BBL × TD model. Contingent on this feature being verified, Eqn 7a could be incorporated within larger-scale models of plant functioning, as is currently done with the BBL model. Although the full model is sufficiently simple to solve numerically, for some practical applications various approximation schemes might also be tested. For example one might set ψ_e to a constant ('perfect homeostasis') so that, through the dependence of [ABA] on J_w in Eqn 8, the ABA-dependent factor in Eqn 7a simplifies to a function of soil and (maximum) xylem hydraulic conductivities (respectively, $1/R_{sr}$ and L_{max}) and of soil water potential (ψ_s). Furthermore, dark respiration might reasonably be ignored in many applications, thus allowing Eqn 11 to be used for the c_i/c_s ratio.

On the theoretical level, a key feature requiring further evaluation is the spatially aggregated description of the mechanical interaction between guard cells and the bulk leaf epidermis (Eqn 3a). This description is currently neither proven nor disproven. As discussed in Appendices 1 and 2, reconciliation of Eqn 3a with the known mechanical advantage of neighbouring subsidiary cells is possible in principle if the guard cell/subsidiary cell complex is mechanically coupled to the rest of the epidermis, for which there is some evidence (Meidner & Edwards 1975). The outcome of this collective mechanical behaviour – as expressed in terms of the relationship between g, P_g and P_e – would depend on the transmission of pressure across the epidermis, and thus on the common areas and elastic properties of the walls dividing neighbouring epidermal cells. Further theoretical justification of the BBL × TD model, incorporating the known mechanical advantage of subsidiary cells, may require a scaling-up analysis of mechanical and osmotic relationships across the epidermis, possibly through extension of the spatially explicit model of hydraulic interactions proposed by Haefner *et al*. (1997).

CONCLUSION

A synthesis and extension of the BBL and TD models has been proposed, which describes combined stomatal responses to air and soil environments. The new model explains a number of common trends reported in the literature, and shows how stomatal regulation of xylem embolism and other processes sensitive to water stress may be achieved through combined hydraulic and chemical signalling in leaves and/or roots. Although over-simplified in many respects, the underlying guard cell picture from which this synthesis has been derived is physiologically meaningful, testable and useful as a guide for further model development. The new model is sufficiently simple to be implemented within plant growth models.

ACKNOWLEDGMENTS

I thank Maurizio Mencuccini, Ray Leuning and Jérôme Ogée for useful comments on this work, and an anonymous reviewer for valuable criticism leading to significant improvement of the manuscript. This work was supported by the European project CARBO-AGE (EVK2 CT 1999 00045).

REFERENCES

Assmann S.M., Snyder J.A., Lee Y.-R.J. (2000) ABA-deficient (*aba1)* and ABA-insensitive (*abi1–1*, *abi2–1)* mutants of *Arabidopsis* have a wild-type stomatal response to humidity. *Plant, Cell and Environment* **23**, 387–395.

Ball J.T., Woodrow I.E., Berry J.A. (1987) A model predicting stomatal conductance and its contribution to the control of photosynthesis under different environmental conditions. In *Progress in Photosynthesis Research*, Vol. IV (ed. I. Biggins), pp. 221–224. Martinus-Nijhoff Publishers, Dordrecht, The Netherlands.

Buckley T.N. & Mott K.A. (2002) Stomatal water relations and the control of hydraulic supply and demand. *Progress in Botany* **63**, 309–325.

von Caemmerer S. & Farquhar G.D. (1981) Some relationships between the biochemistry of photosynthesis and the gas exchange of leaves. *Planta* **153**, 376–387.

Cochard H., Bréda N., Granier A. (1996) Whole tree hydraulic conductance and water loss regulation in *Quercus* during drought: evidence for stomatal control of embolism? *Annales des Sciences Forestières* **53**, 197–206.

Dewar R.C. (1995) Interpretation of an empirical model for stomatal conductance in terms of guard cell function. *Plant, Cell and Environment* **18**, 365–372.

Edwards M., Meidner H., Sheriff D.W. (1976) Direct measurements of turgor pressure potentials of guard cells. *Journal of Experimental Botany* **27**, 163–171.

Farquhar G.D. (1978) Feedforward responses of stomata to humidity. *Australian Journal of Plant Physiology* **5**, 769–772.

Farquhar G.D. & Wong S.C. (1984) An empirical model of stomatal conductance. *Australian Journal of Plant Physiology* **11**, 191–209.

Farquhar G.D., von Caemmerer S., Berry J.A. (1980) A biochemical model of photosynthetic CO_2 assimilation in leaves of C_3 species. *Planta* **149**, 78–90.

Franks P.J., Cowan I.R., Farquhar G.D. (1997) The apparent feedforward response of stomata to air vapour pressure deficit: information revealed by different experimental procedures with two rainforest trees. *Plant, Cell and Environment* **20**, 142–145.

Haefner J.W., Buckley T.N., Mott K.A. (1997) A spatially explicit model of patchy stomatal responses to humidity. *Plant, Cell and Environment* **20**, 1087–1097.

Hartung W. & Davies W.J. (1991) Drought-induced changes in physiology and ABA. In *Abscisic Acid, Physiology and Biochemistry* (eds W.J. Davies & H.G. Jones), pp. 63–79. Bios Scientific Publishers, Oxford, UK.

Hsiao T.C. (1973) Plant response to water stress. *Annual Review of Plant Physiology* **25**, 519–570.

Hubbard R.M., Ryan M.G., Sperry J.S. (2001) Stomatal conductance and photosynthesis vary linearly with plant hydraulic conductance in ponderosa pine. *Plant, Cell and Environment* **24**, 113–121.

Jones H.G. & Sutherland R.A. (1991) Stomatal control of xylem embolism. *Plant, Cell and Environment* **14**, 607–612.

Kearns E.V. & Assmann S.M. (1993) The guard-cell – environment connection. *Plant Physiology* **102**, 711–715.

Korol R.L., Kirschbaum M.U.F., Farquhar G.D., Jeffreys M. (1999) Effects of water status and soil fertility on the C-isotope signature in *Pinus radiata*. *Tree Physiology* **19**, 551–562.

Leuning R. (1990) Modelling stomatal behaviour and photosynthesis of *Eucalyptus grandis*. *Australian Journal of Plant Physiology* **17**, 159–175.

Leuning R. (1995) A critical appraisal of a combined stomatal-photosynthesis model for C_3 plants. *Plant, Cell and Environment* **18**, 339–355.

Magnani F., Mencuccini M., Grace J. (2000) Age-related decline in stand productivity: the role of structural acclimation under hydraulic constraints. *Plant, Cell and Environment* **23**, 251–263.

McMurtrie R.E., Leuning R., Thompson W.A., Wheeler A.M. (1992) A model of canopy photosynthesis and water use incorporating a mechanistic formulation of leaf CO_2 exchange. *Forest, Ecology and Management* **52**, 261–278.

Meidner H. (1975) Water supply, evaporation, and vapour diffusion in leaves. *Journal of Experimental Botany* **26**, 666–673.

Meidner H. & Edwards M. (1975) Direct measurements of turgor pressure potentials of guard cells. I. *Journal of Experimental Botany* **26**, 319–330.

Monteith J.L. (1995) A reinterpretation of stomatal responses to humidity. *Plant, Cell and Environment* **18**, 357–364.

Morison J.I.L. & Gifford R.M. (1983) Stomatal sensitivity to carbon dioxide and humidity. *Plant Physiology* **71**, 789–796.

Mott K.A. (1988) Do stomata respond to CO_2 concentrations other than intercellular? *Plant Physiology* **86**, 200–203.

Mott K.A. & Parkhurst D.F. (1991) Stomatal responses to humidity in air and helox. *Plant, Cell and Environment* **14**, 509–515.

Oren R., Sperry J.S., Katul G.G., Pataki D.E., Ewers B.E., Phillips N., Schfer K.V.R. (1999) Survey and synthesis of intra- and interspecific variation in stomatal sensitivity to vapour pressure deficit. *Plant, Cell and Environment* **22**, 1515–1526.

Pierce M. & Raschke K. (1981) Synthesis and metabolism of abscisic acid in detached leaves of *Phaseolus vulgaris* L. after loss and recovery of turgor. *Planta* **153**, 156–165.

Salleo S., Nardini A., Pitt F., Lo Gullo M.A. (2000) Xylem cavitation and hydraulic control of stomatal conductance in Laurel (*Laurus nobilis* L.). *Plant, Cell and Environment* **23**, 71–79.

Saugier B. & Katerji N. (1991) Some plant factors controlling evapotranspiration. *Agricultural and Forest Meteorology* **54**, 263–277.

Schulze E.-D. (1991) Water and nutrient interactions with plant water stress. In *Response of Plants to Multiple Stresses* (eds H.A. Mooney, W.E. Winner & E.J. Pell), pp. 89–101. Academic Press, San Diego, CA, USA.

Sharpe P.J., Wu H., Spence R.D. (1987) Stomatal Mechanics. In *Stomatal Mechanics* (eds E. Zeiger, G.D. Farquhar & I.R. Cowan), pp. 91–114. Stanford University Press, Stanford, CA, USA.

Sperry J.S. & Pockman W.T. (1993) Limitations of transpiration by hydraulic conductance and xylem cavitation in *Betula occidentalis*. *Plant, Cell and Environment* **16**, 279–287.

Sperry J.S., Adler F.R., Campbell G.S., Comstock J.P. (1998) Limitation of plant water use by rhizosphere and xylem conductance: results from a model. *Plant, Cell and Environment* **21**, 347–359.

Stålfelt M.G. (1966) The role of the epidermal cells in the stomatal movements. *Physiologia Plantarum* **19**, 241–256.

Talbott L.D. & Zeiger E. (1998) The role of sucrose in guard cell osmoregulation. *Journal of Experimental Botany* **49**, 329–337.

Tardieu F. & Davies W.J. (1992) Stomatal response to ABA is a function of current plant water status. *Plant Physiology* **98**, 540–545.

Tardieu F. & Davies W.J. (1993) Integration of hydraulic and chemical signalling in the control of stomatal conductance and water status of droughted plants. *Plant, Cell and Environment* **16**, 341–349.

Tardieu F. & Simonneau T. (1998) Variability among species of stomatal control under fluctuating soil water status and evaporative demand: modelling isohydric and anisohydric behaviours. *Journal of Experimental Botany* **49**, 419–432.

Tardieu F., Lafarge T., Simonneau T. (1996) Stomatal control by fed or endogenous xylem ABA in sunflower: interpretation of observed correlations between leaf water potential and stomatal conductance in anisohydric species. *Plant, Cell and Environment* **19**, 75–84.

Thomas D.S. & Eamus D. (1999) The influence of predawn leaf water potential on stomatal responses to atmospheric water content at constant c_i and on stem hydraulic conductance and foliar ABA concentrations. *Journal of Experimental Botany* **50**, 243–251.

Thornley J.H.M. (1997) Modelling allocation with transport/conversion processes. *Silva Fennica* **31**, 341–355.

Thornley J.H.M. & Johnson I.R. (1990) *Plant and Crop Modelling*. Clarendon Press, Oxford, UK.

Turner N.C., Schulze E.-D., Gollan T. (1985) The response of stomata and leaf gas exchange to vapour pressure deficits and soil water content. II. In the mesophytic herbaceous species *Helianthus annuus*. *Oecologia* **65**, 348–355.

Tyree M.T. & Sperry J.S. (1988) Do woody plants operate near the point of catastrophic xylem dysfunction caused by dynamic water stress? *Plant Physiology* **88**, 574–580.

Tyree M.T. & Yianoulis P. (1980) The site of water evaporation from sub-stomatal cavities, liquid path resistances and hydroactive stomatal closure. *Annals of Botany* **46**, 175–193.

Wilkinson S. & Davies W.J. (1997) Xylem sap pH increase: a drought signal received at the apoplastic face of the guard cell that involves the suppression of saturable abscisic acid uptake by the epidermal symplast. *Plant Physiology* **113**, 559–573.

Wong S.C., Cowan I.R., Farquhar G.D. (1979) Stomatal conductance correlates with photosynthetic capacity. *Nature* **282**, 424–426.

Wu H., Sharpe P.J.H., Spence R.D. (1985) Stomatal mechanics. III. Geometric interpretation of the mechanical advantage. *Plant, Cell and Environment* **8**, 269–274.

Zeiger E., Farquhar G.D., Cowan I.R. (1987) *Stomatal Function*. Stanford University Press, Stanford, CA, USA.

Received 12 January 2002; received in revised form 17 April 2002; accepted for publication 22 April 2002

APPENDIX 1 – RECONCILIATION OF EQN 3A WITH THE MECHANICAL ADVANTAGE OF SUBSIDIARY CELLS

Theoretical and experimental analyses of stomatal mechanics have shown that subsidiary cell turgor (P_s) has a greater (and opposing) influence on stomatal aperture compared with guard cell turgor (P_g):

$$g = \chi_{gs}(P_g - mP_s) \qquad \text{(A1·1)}$$

where m (or more appropriately $m - 1$) is the so-called mechanical advantage of the subsidiary cells ($m > 1$), and χ_{gs} is a mechanical coefficient (Edwards *et al*. 1976; Wu *et al*. 1985; Sharpe *et al*. 1987). Wu *et al*. (1985) showed that m can be related to simple geometric properties of the stomatal apparatus.

In contrast to this local description of stomatal mechanics, the spatially averaged model assumed in the present study (Eqn 3a) has the form

$$g = \chi_{ge}(P_g - P_e) \qquad \text{(A1·2)}$$

where P_e is the turgor pressure of the bulk epidermis. The subscript 'ge' indicates that the value of the spatially aggregated mechanical coefficient χ_{ge} is in general different from the local mechanical coefficient χ_{gs} in Eqn A.1·1.

This Appendix shows that it is possible to reconcile Eqns A1·1 and A1·2 in principle, provided that the guard cells, subsidiary cells and bulk epidermis are mechanically coupled, and that the nature of this coupling takes a particular form. Pressure probe studies have demonstrated that increased turgor in cells other than neighbouring subsidiary cells can cause partial stomatal closure (Meidner & Edwards 1975). If the nature of this mechanical coupling is such that the spatially averaged turgor pressures are related by

$$mP_s = (1-r)P_g + rP_e \qquad \text{(A1·3)}$$

for some constant r, then Eqns A1·1 and A1·2 are equivalent, their respective mechanical coefficients being related through

$$\chi_{ge} = r\chi_{gs} \qquad \text{(A1·4)}$$

as may be verified by direct substitution. Two further conditions are required for consistency. First, Eqn A1·3 implies that if P_s is to remain positive throughout the range $0 < P_e < P_g$ then we must have $r < 1$. Secondly, for water to flow from the bulk epidermis towards the subsidiary cells requires that $\psi_s < \psi_e$, implying that

$$\Delta\pi_{se} = \pi_s - \pi_e > P_s - P_e = \frac{(1-r)P_g - (m-r)P_e}{m} \qquad \text{(A1·5)}$$

where we have used Eqn A1·3. In the subrange $0 < P_e < P_g(1-r)/(m-r)$ where the turgor difference $P_s -$

P_e is positive, we therefore require that the osmotic gradient $\Delta\pi_{se}$ is sufficiently large and positive. In the derivation of the BBL × TD model from Eqn A1·2, π_e was assumed to be a fixed parameter; this does not exclude the possibility that π_s is larger than π_e and thus that Eqn A1·5 can be satisfied.

In summary, consistency between the two mechanical models of stomatal conductance is possible in principle, provided that the mechanical coupling between the average turgor pressures of the guard cells, subsidiary cells and bulk epidermis takes the form of Eqn A1·3 for some $r < 1$, and that there is a sufficiently positive osmotic pressure gradient from the bulk epidermis to the subsidiary cells. Establishing the validity or otherwise of these conditions would require further theoretical and/or experimental information on the spatial distribution of cell pressure-volume relations and osmotic gradients across the epidermis.

APPENDIX 2 – PROSPECTS FOR A 'BOTTOM-UP' EXPLANATION OF THE BBL AND TD MODELS

The main motivation for adopting the spatially aggregated description of stomatal mechanics (Eqn 3a) for this study has been that it is mathematically consistent with the BBL and TD models. Complementary to this 'top-down' approach to stomatal mechanics, one would like to explain the BBL and TD models from a 'bottom-up' approach based directly on a local description of the known mechanical advantage of subsidiary cells. Haefner *et al*. (1997) proposed a spatially explicit model of hydraulic interactions across the leaf, consisting of a rectangular grid of stomatal units (guard cells and surrounding epidermal tissue) grouped into areoles surrounded by veins. The stomatal conductance of each grid was modelled using Eqn A1·1:

$$g = \chi_{gs}(P_g - mP_s) \tag{A2·1}$$

where P_g and P_s represent the local turgor pressures of, respectively, the guard cells and surrounding epidermal tissue within the grid. Water flows between grid points in response to the local water potential gradient. Haefner *et al*. assumed that local pumping of solutes into guard cells was proportional to P_s. This Appendix discusses the prospects for such a model to explain the empirical BBL and TD models.

Assuming that the guard cells are in local hydraulic equilibrium with the surrounding epidermal tissue within each stomatal unit ($\psi_g = \psi_s$), it is straightforward to show from Eqn A2·1 that

$$g = \chi_{gs}\{\pi_g - \pi_s - (m-1)P_s\} \tag{A2·2}$$

The ion pumping assumption proposed by Haefner *et al*. (1997) implies that

$$\frac{d\pi_g}{dt} = \mu_0 P_s - d(\pi_g - \pi_s) \tag{A2·3}$$

where μ_0 is a pumping coefficient (cf. main text Eqn 5a). Haefner *et al*. assumed that the value of π_s was a fixed constant across the leaf. Combining Eqns A2·2 and A2·3 in the steady state then gives

$$g = \chi_{gs}\left(\frac{\mu_0}{d} - m + 1\right)P_s \tag{A2·4}$$

Within a simple one-dimensional approximation to water flow (as used in the present model based on Eqn A1·2), we have

$$P_s = P_v - \frac{E}{K_{vs}} = P_v - \frac{1{\cdot}6D_s g}{K_{vs}} \tag{A2·5}$$

where P_v is the vein turgor pressure (which was assumed fixed), K_{vs} is the hydraulic conductivity between the veins and the guard cells, and we have used Eqn 6c. Combining Eqns A2·4 and A2·5 then gives, after rearranging,

$$g = \frac{\chi_{gs}\left(\frac{\mu_0}{d} - m + 1\right)P_v}{1 + \frac{1{\cdot}6D_s\chi_{gs}}{K_{vs}}\left(\frac{\mu_0}{d} - m + 1\right)} \tag{A2·6}$$

Therefore, in this simple one-dimensional approximation, Haefner *et al*.'s model predicts a stomatal response to air humidity deficit (D_s) that has the same mathematical form as that of the BBL model (Eqn 1). However g is a saturating function of μ_0/d. If the responses to leaf irradiance, CO_2 and soil humidity were to enter through the pumping coefficient μ_0 and diffusion coefficient d (e.g. via ATP and ABA in analogy with the present model), then we would not obtain the simple multiplicative form of the BBL × TD model (cf. Eqn 7a), and would lose the associated homeostatic behaviour of the c_i/c_s ratio and leaf water potential. For example, if μ_0 were proportional to $(A_n + R_d)/c_i$ (cf. Eqn 5c) then g would not be proportional to $(A_n + R_d)/c_i$, resulting in a more variable c_i/c_s ratio.

This simplified analysis does not exclude the possibility that the BBL and TD models can be explained using the full two-dimensional version of Haefner *et al*.'s model, with an alternative prescription for the pumping parameter μ_0, and/or with a spatially varying (rather than constant) value of π_s. Appendix 1 suggests that mechanical interactions across the leaf epidermis may also need to be represented.

APPENDIX 3 – THE DEPENDENCE OF THE MINIMUM FOLIAGE WATER POTENTIAL ($\psi_{e,min}$) ON THE MODEL PARAMETERS

Here we calculate the value of ψ_e at the lowest turning point in the $\psi_e - \psi_s$ plot (Fig. 4b), in the limit of saturating light ($Q \to \infty$). In this limit, the stomatal conductance model (Eqn 7a) simplifies because $(A_n + R_d)/c_i \to g_x$ (see Eqn 10c), and the steady-state water balance relationship (Eqn 12a) then gives

$$J_w = \frac{1{\cdot}6D_s a_1 g_x}{1 + \frac{D_s}{D_0}}\exp\{-[\mathrm{ABA}]\beta\exp(\delta\psi_e)\}. \tag{A3·1}$$

At the minimum of the $\psi_e - \psi_s$ plot, a small change in ψ_s leads to an equal change in both sides of Eqn A3·1, and no

change in ψ_e. If $\partial/\partial\psi_s$ denotes a partial rate of change with respect to ψ_s at constant ψ_e, then applying $\partial/\partial\psi_s$ to Eqn A3·1 at the minimum gives

$$\frac{\partial J_w}{\partial \psi_s} = -J_w \beta \exp(\delta\psi_e)\frac{\partial [\mathrm{ABA}]}{\partial \psi_s}, \tag{A3·2}$$

and $\psi_{e,min}$ is then the value of ψ_e that satisfies this condition. From Eqn 8 (in which we make the approximation $a << J_w$, and substitute $\psi_r = \psi_e + J_w R_{re}$) we have

$$[\mathrm{ABA}] = \frac{-(\lambda_r + \lambda_e)\psi_e}{V_w J_w} - \frac{\lambda_r R_{re}}{V_w}, \tag{A3·3}$$

so that

$$\begin{aligned}\frac{\partial [\mathrm{ABA}]}{\partial \psi_s} &= \frac{1}{{J_w}^2}\frac{\partial J_w}{\partial \psi_s}\frac{(\lambda_r + \lambda_e)\psi_e}{V_w} \\ &= -\frac{1}{J_w}\frac{\partial J_w}{\partial \psi_s}\left([\mathrm{ABA}] + \frac{\lambda_r R_{re}}{V_w}\right),\end{aligned} \tag{A3·4}$$

where in the second step we have re-used Eqn A3·3. Substituting Eqn A3·4 into Eqn A3·2 and noting some cancellations, we find

$$\begin{aligned}1 &= \beta \exp(\delta\psi_e)\left([\mathrm{ABA}] + \frac{\lambda_r R_{re}}{V_w}\right) \\ &= -\beta \exp(\delta\psi_e)\frac{(\lambda_r + \lambda_e)\psi_e}{V_w J_w},\end{aligned} \tag{A3·5}$$

(second step using Eqn A3·3 again). Using the first equality in Eqn A3·5 to eliminate [ABA] from Eqn A3·1, we have

$$J_w = \frac{1{\cdot}6 D_s a_1 g_x}{1 + \dfrac{D_s}{D_0}} \exp\left\{-1 + \frac{\lambda_r \beta \exp(\delta\psi_e) R_{re}}{V_w}\right\}. \tag{A3·6}$$

Finally, Eqn A3·6 can then be used to eliminate J_w from the last part of Eqn A3·5. We then find after rearrangement:

$$-\psi_e \exp(\delta\psi_e) = \Omega \exp\left\{\frac{\lambda_r \beta \exp(\delta\psi_e) R_{re}}{V_w}\right\}, \tag{A3·7}$$

where Ω is the parameter combination

$$\Omega = \frac{1{\cdot}6 D_s a_1 g_x}{1 + \dfrac{D_s}{D_0}} \frac{V_w \exp(-1)}{\beta(\lambda_r + \lambda_e)}. \tag{A3·8}$$

Eqn A3·7 is an implicit equation for ψ_e, the solution of which ($\psi_{e,min}$) may be obtained numerically. In the default case where ABA is synthesized in leaves only ($\lambda_r = 0$, $\lambda_e > 0$), Eqn A3·7 reduces to

$$-\psi_e \exp(\delta\psi_e) = \Omega, \tag{A3·9}$$

and Eqn A3·8 reduces to

$$\Omega = \frac{1{\cdot}6 D_s a_1 g_x}{1 + \dfrac{D_s}{D_0}} \frac{V_w \exp(-1)}{\beta \lambda_e}. \tag{A3·10}$$

In this case therefore the minimum leaf water potential depends on just two parameters: δ and Ω. Finally, the absolute lowest value of $\psi_{e,min}$ occurs in the limit of high VPD ($D_s \to \infty$), when the expression for Ω reduces further to

$$\Omega = \frac{\mu K g_x V_w \exp(-1)}{d_{min} \beta \lambda_e}, \tag{A3·11}$$

where we have used Eqns 7b and 7c of the main text to substitute for a_1 and D_0.